USE SIGNAL TO NOISE RATIO DATA OF RADIO OCCULTATION TECHNIQUE TO DETECT LOWER IONOSPHERE

Wen-Hao Yeh[1], Cheng-Yung Huang[2], Tsen-Chieh Chiu[1], Yuei-An Liou[3]

[1]Department of Electrical Engineering, NCU, Taiwan
965401015@cc.ncu.edu.tw
[2]GPS Science and Application Research Center, NCU, Taiwan
[3]Center for Space and Remote Sensing Research, NCU, Taiwan

ABSTRACT

Radio occultation (RO) technique has been used to investigate planetary atmosphere since 1960s to 1970s. With the advent of global positioning system (GPS), it has been used to do the research of Earth's atmosphere. Taiwan has launched six low Earth orbit satellites as a RO constellation mission, named FOMOSAT-3/COSMIC (F-3). F-3 mission release data per day is 1500 to 2500 set for neutral atmosphere. The coverage of the data is from near surface to several tens more than 100 km in altitude and position is global distributed. In signal to noise ratio (SNR) data, one third to half has the perturbation near 100 km in altitude, which is the ionospheric E and F region occurring altitude. In this study, the relation between lower ionosphere and perturbation is simulated by using ray tracing method based on geometrical optics. Furthermore, the analysis method of the perturbation data is developed and the distribution of the perturbation is constructed with the global coverage of the RO data.

KEY WORDS: GPS, Radio Occultation, FORMOSAT-3, Ionosphere

1. INTRODUCTION

The mid –latitude sporadic E (Es) layers are the thin layers of metallic ion plasma and form at E region heights between 95 and 125 km and it have been studied for many years (Whitehead, 1970; Whitehead, 1989; Mathews, 1998). The physics of Es formation is based on the "wind shear" theory, in which vertical shears in the horizontal neutral wind can cause, by the combined action of ion-neutral collisional coupling and geomagnetic Lorentz forcing, the long-lived metallic ions to move vertically and converge into thin and dense plasma layers (Haldoupis et al. 2006).

Es have been observed by ionosondes, incoherent scatter radars, or other radio methods as backscatter radars. The disadvantages of upper technique only can observe Es layers in local area. In 1990s, radio occultation (RO) technique has been used to do the research of Earth's atmosphere. The observation of by using RO technique is used to do research of Es layers. The diagram of RO technique is shown in Figure 1. In Figure 1, GPS satellite is set at the position of point A. When the GPS signal propagates through atmosphere, it will be bended by the gradient of refractive index and then received by LEO satellite which is set at the position of point B. Hocke et al. (2001) have used the difference of the phase of GPS L1 and L2 signal to obtain the ionospheric irregularities. Wu et al. (2005) have used the scintillations of phase and SNR of RO data to obtain the morphology of Es layers. Chu et al. (2011) have used retrieval electron density to compare with other observation results to determine the coordinate of Es layer.

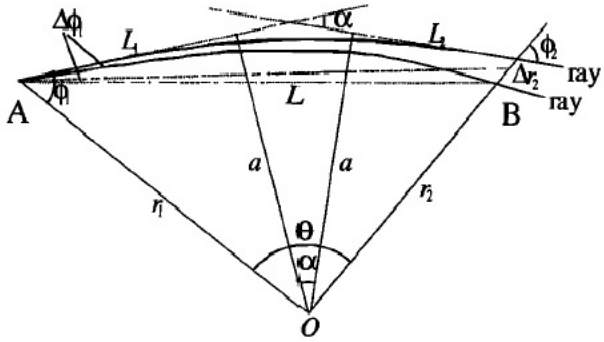

Figure 1. A layout of rays propagate between transmitter A and receiver B in a spherically symmetric atmosphere. (Sokolovskiy, 2000)

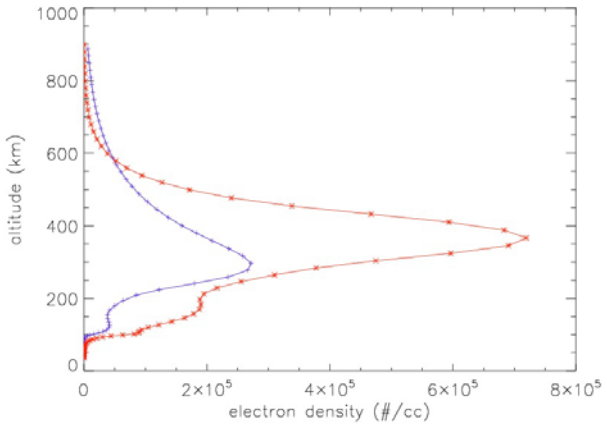

Figure 2. Day time (red) and night time(blue) electron density profile from TIEGCM model.

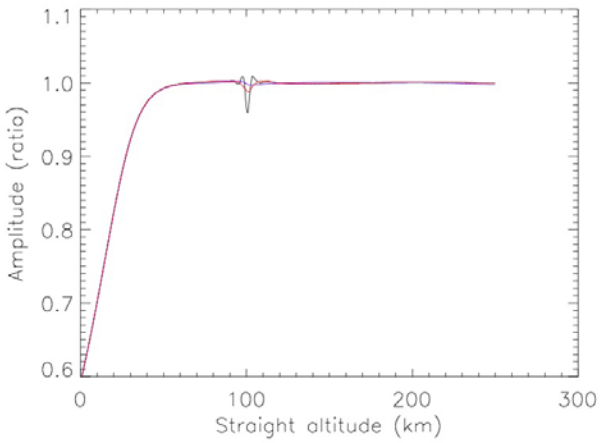

Figure 3. Simulation results of amplitude.

In this study, the relation between electron density and fluctuation of SNR of RO data is simulated by ray tracing method to compare with the observational RO data. Furthermore, the method to analyse the observational SNR of RO data is developed. The simulation method is summarized in Section 2. In Section 3, the comparison between simulation results and observational data are described. The analysis method of observational results is in Section 4. And followed are analysis results and conclusions.

2. AMPLITUDE SIMULATION BY USING RAY TRACING METHOD

2.1 Ray tracing method

The ray tracing method in this research is based on geometric optics and cited from Yeh et la (2012). The relation between the position vector and refractive index is given by Born and Wolf (1999) is used the differential equation of light rays

$$\frac{d}{ds}\left(n\frac{d\vec{r}}{ds}\right)=n\frac{d^2\vec{r}}{ds^2}+\frac{dn}{ds}\frac{d\vec{r}}{ds}=\nabla n, \qquad (1)$$

where n, ds, $d\vec{r}$ are the refractive index, the path length, and the position vector of the signal trajectory, to calculate the ray path. In this work, we transform equation (1) as bellow:

$$\frac{d^2\vec{r}}{ds^2}=\frac{1}{n}\left[\nabla n-\frac{dn}{ds}\frac{d\vec{r}}{ds}\right]. \qquad (2)$$

Then the trajectory of the signal can be integrated by using Range-Kutta method if the refractive index of the intermediate is known.

2.2 Refractive index of ionosphere & atmosphere

In atmosphere, the refractive index is controlled by electron density, pressure, temperature, and moisture. In order to simplify the simulation, the refractive index in this study is controlled by electron density and neutral atmosphere refractivity. The relation between electron density and refractive index is followed from Appleton-Hartree formula

$$n^2=1-\frac{X}{1-iZ-\frac{Y_T^{\,2}}{2(1-X-iZ)}\pm\sqrt{\frac{Y_T^{\,4}}{4(1-X-iZ)}+Y_L^{\,2}}} \qquad (3)$$

where $z=\nu/f$, f is GPS signal frequency, ν is electron collision frequency, Y_T, Y_L are related to the magnetic field with reference to the direction of the wave normal, and $X=f_N/f$, where $f_N\cong 80.62N_e$ is a measurement of electron motion around the heavy ion and proportional to electron density (N_e). The simply equation (3) becomes

$$n=1-\frac{40.31}{f^2}N_e \qquad .$$

(4)

The refractive index in neutral atmosphere is only for conformation the practical RO signal propagation. The profile of neutral atmospheric refractive index is

$$N(h)=400\exp\left(\frac{-h}{8}\right), \qquad (5)$$

where h is the altitude in km.

2.3 Amplitude simulation

The amplitude of the ray tracing simulation signal is followed from Sokolovskiy (2000). The diagram of the amplitude calculation is shown in Figure 1. In Solilovskiy (2000), the energy flux (square of amplitude A) K is

$$K=\left|\frac{A}{A_0}\right|^2=\left|\frac{L\Delta\phi_1}{\Delta r_2\sin\phi_2}\right|, \qquad (6)$$

where A_0 is the reference amplitude. From equation (6), the energy flux is related to the cross section of the ray cone. In the two dimensional simulation in this research, two nearby signal trajectory can be regarded as a ray cone. The cross section of the ray cone in this research is the cross section of two nearby end points of two nearby simulation trajectories. Then the amplitude ratio of the simulation signal can be obtained. The A_0 in the simulation is the amplitude of the highest signal trajectory.

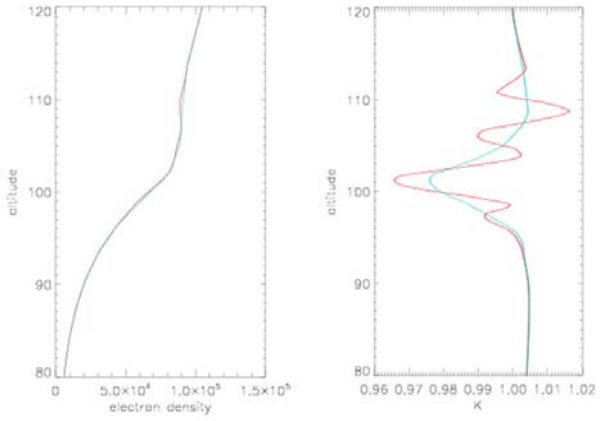

Figure 4. Simulation results of perturbation in electron density profile.

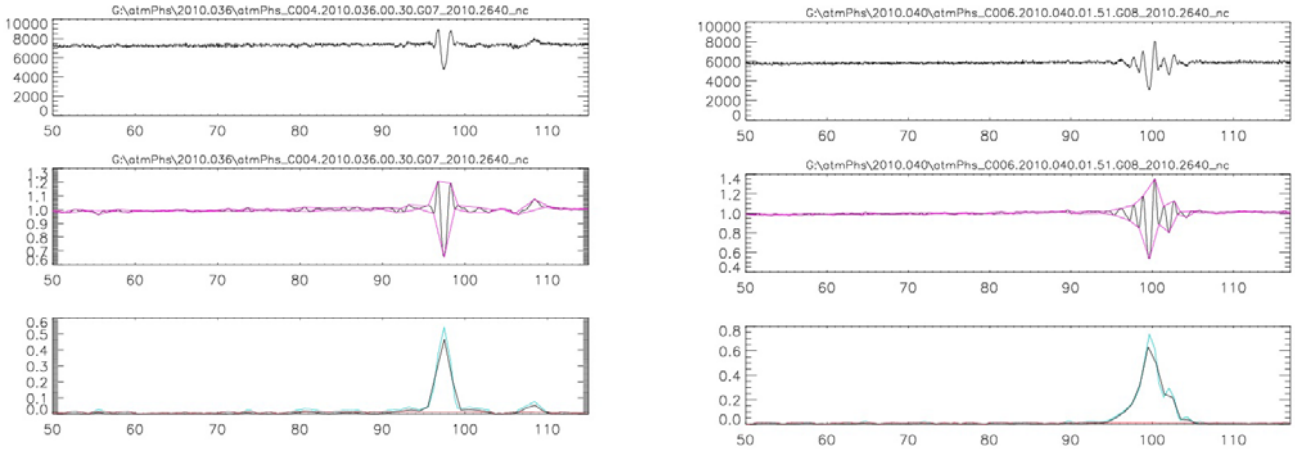

(a) (b)

Figure 5. The observation SNR data and the diagram of data analysis method.

3. THE COMPARISON BETWEEN SIMULATION AND OBSERVATIONAL AMPLITUDE RESULTS OF LOWER IONOSPHERE

The simulations with the spherically symmetric electron density profiles in Figure 2 and neutral atmosphere refractive index of equation (1) are shown in Figure 3. The decay phenomena at the left side of three curves are caused by the refractive index profile of neutral atmosphere. The blue and red curves in Figure 3 are corresponded to the electron density profiles in Figure 2. In Figure 3, a very slight negative hump at 100 km of blue curve and 135 km of red curve. These humps are caused by the peaks at the about 180 km of day time and 120 km of night time electron density profiles in Figure 2. The obvious peak of red curve in Figure 3 is caused by the small hump at about 100 km of day time electron density profile in Figure 2. The peak of black curve in Figure 3 is caused by the same electron profile of red curve but the magnitude of the small hump is larger.

In the electron density profile, the local minimum is like a convex lens to focus the signal and the local maximum is like a concave lens to scatter the signal. So the minus peak is made by the concave lens effect of the local maximum of the small hump. And the two equal magnitude peaks near the minus peak are made by the convex lens effect of the local minimum near the local maximum.

Furthermore, the electron density profile of ionosphere is not always so clear like the profiles in Figure 2. We add a perturbation in the small hump near 100 km on the day time electron profile in Figure 2. The profile with perturbation is shown in the left plot in Figure 4. The blue curve is the original profile and the red one is the perturbation. The simulation results are shown in the right plot in Figure 4 and the perturbations of the simulation result is obviously and correspond to the perturbation in the electron density profile.

In the top plot of Figure 5a and 5b are two SNR data of RO observations. In the top plot of Figure 5a, a minus peak occurs at about 100 km and the shape likes the minus peak of black curve in Figure 3. And in the top plot of Figure 5b, a perturbation around 90 km and it presume the perturbation is caused by the perturbation in the electron density profile like in the left plot in Figure 4.

4. ANALYSIS METHOD OF OBSERVATIONAL RO DATA

With the simulation results in Section 3, the electron density variation will reflect on the propagating signal amplitude variation. In this section is the method to analysis the variation of the RO amplitude data.

The lowest of the altitude is down to 50 km. The first step of the analysis procedure is to smooth and normalize the SNR data. In the top plot of Figure 5a and 5b, the raw SNR data contains vibration. In order not be affected by the vibration in the following steps, a constrained matrix smoothing method used in Feng & Herman (1999) is used to smooth the SNR data. The smoothed and normalized SNR data are the black curved in the middle plots of Figure 5a and 5b.

The second step is to quantify the variation. In this step, we use the idea of empirical mode decomposition (EMD) method to do quantification. The purple lines in the middle plots of Figure 5a and 5b are the upper and lower boundary of the black curves. The variation is the value of upper boundary minus lower boundary and shown in the blue curves in the lower plots in Figure 5a and 5b.

The third step is to remove the background variation. When the GPS signal propagates the atmosphere, it may be affected by some other influence in the atmosphere. In order to remove the influence, the back ground variation need to be removed to manifest the main variation. The background in this research is made by the half lowest value of the variation degree which are the red curves in the lower plots in Figure 5a and 5b. The variation degree

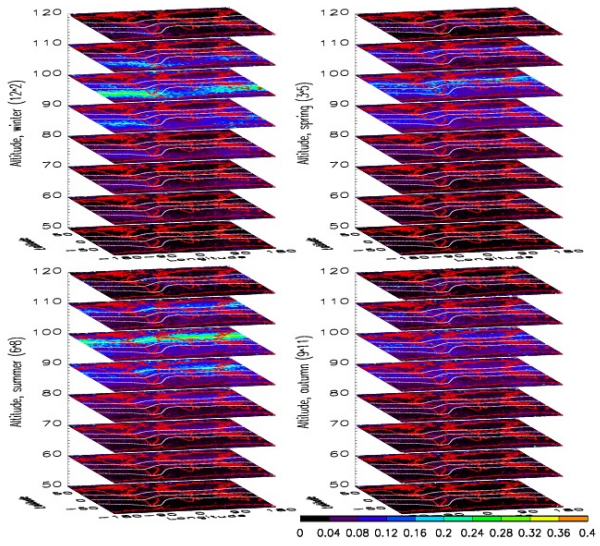

Figure 6. Analysis result of observational SNR of RO data.

is the black line which defined as the value of the blue line minus the red line in Figure 5a and 5b.

5. ANALYSIS RESULT AND CONCLUSIONS

We analyse the SNR data in 2010 and separate them into four seasons. The distributions of the variation degree in four seasons are shown in Figure 6. In Figure 6, the higher value of variation degree is appears in the range from 90 km to 110 km in altitude. The white lines in Figure 6 are the equator and 30˚N and 30˚S of geomagnetic coordinate. The variation degree has a great increase in the range from 90 km to 110 km and has the maximum near 100 km in altitude. Generally speaking, the maximum of variation degree in winter and summer is greater than in spring and autumn. And in spring is greater than in autumn and distribute near the equator of geomagnetic coordinate. In winter, the maximum of variation degree follows the 30˚S, and in summer the maximum of variation degree follows the 30˚N. It may be caused by the irradiation of solar radiation.

Acknowledgements

The authors would thank Prof. Hsiao Tung-Yuan, Department of Information Technology, Hsing-Wu Institute of Technology, to give great opinions of this research.

References from Journals:

Born M., and E. Wolf, 1999. *Principles of Optics: Electromagnetic Theory of Propagation, Interference and Diffraction of Light.* 7th (expanded) edition Cambridge University Press, New York

Chu, Y.-H., P. S. Brahmanandam,C.-Y. Wang, C.-L. Su, R.-M. Kuong. 2011. Coordinated sporadic E layer observations made with Chung-Li 30 MHz radar, ionosonde and FORMOSAT-3/COSMIC satellites. *Journal of Atmospheric and Solar-Terrestrial Physics*, 73, pp. 883-894.

Feng D. D. and M. Herman, 1999. Remote Sensing the Earth's Atmosphere Using the Global positioning System (GPS) — The GPS/MET Data Analysis, *J. Atmos. Oceanic Technol.*, 16, 989.

Haldoupis, C, C. Meek, N. Christakis, D. Pancheva, A. Bourdillon, 2006. Ionogram height-time-intensity observations of descending sporadic E layers at mid-latitude. *Journal of Atmospheric and Solar-Terrestrial Physics*, 68, pp. 539-557.

Hocke, K., K. Igarashi, M. Nakamura, P. Wilkinson, J. Wu, A pavelyev, J. Wickert. 2001. Global sounding of sporadic E lyers by the GPS/MET radio occultation experiment. *Journal of Atmospheric and Solar-Terrestrial Physics*, 63, pp. 1973-1980.

Mathews, J. D. 1998. Sporadic E: current views and recent progress. *Journal of Atmospheric and Solar-Terrestrial Physics*, 60(4), pp. 413-435.

Sokolovskiy, S.V. 2000. Inversions of radio occultation amplitude data. *Radio Science*, 35(1), pp. 97-105.

Whitehead, J. D. 1970. Production and prediction of sporadic E. *Reviews of Geophysics and Space Physics*, 8, pp. 65-144.

Whitehead, J. D. 1989. Recent work on mid-latitude and equatorial sporadic E. *Journal of Atmospheric and Solar-Terrestrial Physics*, 51, pp. 401-424.

Wu, D. L., C. O. Ao, G. A. Hajj, M. T. Juarez, A. J. Mannucci. 2005. Sporadic E morphology from GPS-CHAMP radio occultation. *Journal of Geophysical Research*, 110, A01306.

Yeh, W.-H., M.-Q Chen, T.-C. Chiu, C.-Y. Huang, Y.-A. Liou, 2012. Ray tracing simulations in nonspherically symmetric atmosphere for GPS radio occultation. will submit to *GPS Solutions*.